

See discussions, stats, and author profiles for this publication at: <https://www.researchgate.net/publication/228439486>

Liquid–Liquid Equilibrium of Cholinium–Derived Bistriflimide Ionic Liquids with Water and Octanol

ARTICLE *in* THE JOURNAL OF PHYSICAL CHEMISTRY B · JULY 2012

Impact Factor: 3.3 · DOI: 10.1021/jp3053168 · Source: PubMed

CITATIONS

13

READS

73

7 AUTHORS, INCLUDING:



Isabel Marrucho

New University of Lisbon

250 PUBLICATIONS 6,967 CITATIONS

SEE PROFILE



José Esperança

New University of Lisbon

110 PUBLICATIONS 4,491 CITATIONS

SEE PROFILE



Jose Nuno A Canongia Lopes

Technical University of Lisbon

179 PUBLICATIONS 8,342 CITATIONS

SEE PROFILE

Liquid–Liquid Equilibrium of Cholinium-Derived Bistriflimide Ionic Liquids with Water and Octanol

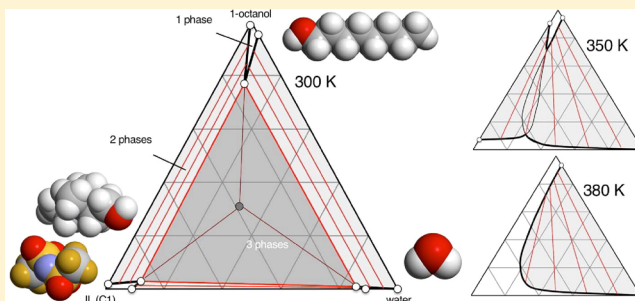
Anabela J. L. Costa,[†] Mário R. C. Soromenho,[†] Karina Shimizu,^{†,‡} Isabel M. Marrucho,[†] José M. S. S. Esperança,^{*,†} J. N. Canongia Lopes,^{*,†,‡} and Luís Paulo N. Rebelo[†]

[†]Instituto de Tecnologia Química e Biológica, Universidade Nova de Lisboa, Av. República, 2780-157 Oeiras, Portugal

[‡]Centro de Química Estrutural, Instituto Superior Técnico, 1049-001 Lisboa, Portugal

S Supporting Information

ABSTRACT: The liquid–liquid equilibria of mixtures of cholinium-based ionic liquids (*N*-alkyl-*N,N*-dimethylhydroxyethylammonium bis(trifluoromethane)sulfonylimide, $[N_{1+n}2OH][Ntf_2]$, $n = 1, 2, 3, 4$, and 5) plus water or 1-octanol were investigated at atmospheric pressure over the entire composition range. The experiments were conducted between 265 and 385 K using the cloud-point method. The systems exhibit phase diagrams consistent with the existence of upper critical solution temperatures. The solubility of $[N_{1+n}2OH][Ntf_2]$ in water is lower for cations with longer alkyl side chains (larger n values). The corresponding trend in the octanol mixtures is reversed. The $([N_{1+n}2OH][Ntf_2] + \text{water} + \text{octanol})$ ternary system shows triple liquid–liquid immiscibility at room temperature and atmospheric pressure. A combined analytic/synthetic method was used to estimate the corresponding phase diagram under those conditions. Auxiliary molecular dynamics simulation data were used to interpret the experimental results at a molecular level.



INTRODUCTION

Choline, also known as cholinium chloride, is the salt combining the *N,N,N*-trimethylhydroxyethylammonium cation, $[N_{1112OH}]^+$, with the chloride anion. It is classified as an essential nutrient for humans and some studies support the view that the presence of this salt is crucial for several biological functions.¹ A diet that includes choline is especially important during pregnancy and lactation time due to its critical role in brain development and memory functions.^{2,3}

The use of cholinium-based ionic liquids as less toxic and more biodegradable alternatives to other more traditional ionic liquids⁴ does not compromise most of the remarkable properties of ionic liquids, namely their wide liquid range, nonflammability, or negligible vapor pressure at ambient conditions.^{5–8} Nevertheless, cholinium-based ionic liquids tend to show higher melting points than analogous ionic liquids based on the ubiquitous 1-alkyl-3-methylimidazolium cation.⁹ The choice of the bis(trifluoromethanesulfonyl)imide anion, $[Ntf_2]^-$, as counterion can minimize this problem ($[Ntf_2]$ -based ionic liquids tend to have lower melting points than similar ionic liquids based on other anions). On the other hand, breaking the symmetry of the cholinium cation by replacing one of the methyl groups by a longer alkyl chain ($[N_{1+n}2OH]^+$ instead of $[N_{1112OH}]^+$) also reduces the melting point temperature of the corresponding ionic liquids. However, it must be stressed that these options (a cholinium-based ionic liquid family with $[Ntf_2]^-$ anions and long alkyl side chains) can compromise the status of these ionic liquids as nontoxic

compounds.^{10,11} from the available studies that focus on the toxicity and biodegradability of cholinium-based ionic liquids with distinct anions,^{12–16} there is one¹³ that presents toxicity data for the bistriflimide anion and confirms the increased toxicity of those ionic liquids when compared to the analogous halide-based compounds.

The recent interest in cholinium-based ionic liquids can be attested by the number of studies concerning possible applications of these compounds, namely in catalytic reactions,^{17–21} as reaction media,²² in processing of metals and metal oxides,²³ as cross-linking agents,²⁴ or as emulsion stabilizing agents.²⁵

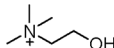
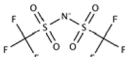
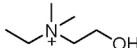
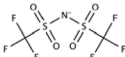
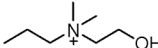
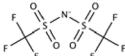
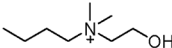
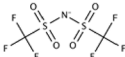
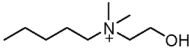
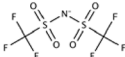
The fluid phase equilibria of binary systems studies involving ionic liquids and molecular solvents have been extensively investigated.^{26–31} Most of these studies include ionic liquids based on 1-alkyl-3-methylimidazolium cations and it has been observed that many of the corresponding phase diagrams show liquid–liquid demixing phenomena capped by the existence of upper critical solution temperatures (UCSTs). In the case of ionic liquid plus 1-alkanol binary mixtures, larger alkanols exhibit higher UCST values whereas ionic liquids with longer alkyl side chains show lower UCST values (or even complete miscibility) with some 1-alkanols in the studied temperature ranges.^{32–34} In the case of ionic liquid plus water binary

Received: May 31, 2012

Revised: July 6, 2012

Published: July 9, 2012

Table 1. Name, Acronym, and Structural Formula of the Ionic Liquids Studied in This Work

Ionic Liquid	Acronym	Cation	Anion
<i>N,N,N</i> -trimethyl- <i>N</i> -(2-hydroxyethyl)ammonium bis(trifluoromethanesulfonyl)imide	[N _{1 1 1} 2OH] [Ntf ₂]		
<i>N</i> -ethyl- <i>N,N</i> -dimethyl- <i>N</i> -(2-hydroxyethyl)ammonium bis(trifluoromethanesulfonyl)imide	[N _{1 1 2} 2OH] [Ntf ₂]		
<i>N</i> -propyl- <i>N,N</i> -dimethyl- <i>N</i> -(2-hydroxyethyl)ammonium bis(trifluoromethanesulfonyl)imide	[N _{1 1 3} 2OH] [Ntf ₂]		
<i>N</i> -butyl- <i>N,N</i> -dimethyl- <i>N</i> -(2-hydroxyethyl)ammonium bis(trifluoromethanesulfonyl)imide	[N _{1 1 4} 2OH] [Ntf ₂]		
<i>N</i> -pentyl- <i>N,N</i> -dimethyl- <i>N</i> -(2-hydroxyethyl)ammonium bis(trifluoromethanesulfonyl)imide	[N _{1 1 5} 2OH] [Ntf ₂]		

mixtures, the opposite trend is usually found: UCSTs tend to increase for longer alkyl side chains in the ionic liquid.^{35,36} Very few studies regarding the phase behavior of binary or ternary mixtures of cholinium-based ionic liquids with molecular solvents have been completed^{37–40} and just one of them⁴⁰ focuses on the effect (in SLE) of increasing the alkyl chain length in the cholinium cation in bromide-based salts. The binary systems studied so far based on the [Ntf₂][−] anion include the [N_{1 1 1} 2OH][Ntf₂] plus water³⁷ and [N_{1 1 2} 2OH][Ntf₂] plus water and 11 other molecular solvents.³⁸

In this work, we have systematically studied the liquid–liquid phase behavior of mixtures of [N_{1 1 *n*} 2OH][Ntf₂] ionic liquids (*n* = 1, 2, 3, 4, and 5) with water or 1-octanol. The two chosen molecular solvents are relevant in the context of chemical, pharmacological, or biological sciences due to their extensive use in the definition of water–octanol partition or distribution coefficients that give a measure of the hydrophilic or hydrophobic nature of a given compound.

EXPERIMENTAL SECTION

Chemicals. All *N*-alkyl-*N,N*-dimethylhydroxyethylammonium bistriflimide ionic liquids, [N_{1 1 *n*} 2OH][Ntf₂] (*n* = 1, 2, 3, 4, and 5), used in this work were synthesized in-house according to previously described synthetic routes.⁴¹ The structural formula of each compound, the corresponding acronym, and final purity are presented in Table 1. The proton NMR analyses of all ILs (recorded with a BRUKER Avance 400 Ultrashield Plus spectrometer) are given as Supporting Information. Immediately prior to their use, all ionic liquid samples were thoroughly dried/degassed under vacuum (0.1 Pa), moderate temperature (330 K), and vigorous stirring

conditions for periods longer than 1 day. Coulometric Karl Fischer titrations yielded final water contents below 300 ppm.

Experimental Setup and Method. Liquid–liquid phase equilibrium (LLE) measurements were carried out at atmospheric pressure using a method based on the visual detection of the turbidity of solutions contained in 4 mL Pyrex glass cells equipped with magnetic stirrers. The solutions were gravimetrically prepared directly inside the cells using an analytical high-precision balance with an uncertainty of 20 μg (corresponding to mixture compositions with errors below 0.0005 mass fraction in most cases). In each separate experimental run the cell was immersed in a thermostatic bath and the sample was continuously stirred until the occurrence of the phase transition was detected. A water–ethylene glycol bath was used for measurements between 293 and 333 K; a silicone oil bath was used for measurements between 333 and 430 K. The temperature of the liquid–liquid phase transition was taken at the point in which the first sign of turbidity appeared in the homogeneous solution upon cooling. Data were then confirmed by repeated cooling–heating cycles (three in most cases). The temperature was monitored using a four-wire platinum resistance thermometer coupled to a Keithley 199 System DMM/Scanner multimeter with a precision better than 0.01 K.

The estimated overall uncertainty due to the use of a dynamic visual method coupled with a small-scale experimental setup is 0.5 K in temperature.

The LLE of two ternary mixtures of ([N_{1 1 1} 2OH][Ntf₂] + water + 1-octanol) and ([N_{1 1 5} 2OH][Ntf₂] + water + 1-octanol) were also studied at room temperature.

Table 2. Experimental LLE Cloud-Point Temperatures of ($[N_{11n2OH}][Ntf_2]$ (IL) Plus Water) Mixtures at Atmospheric Pressure

W_{IL}	X_{IL}	T/K	W_{IL}	X_{IL}	T/K	W_{IL}	X_{IL}	T/K
$[N_{1112OH}][Ntf_2]$ + Water								
0.090	0.005	288.1	0.239	0.015	336.5	0.653	0.081	344.5
0.102	0.005	299.1	0.294	0.019	341.8	0.732	0.113	340.0
0.118	0.006	307.5	0.365	0.026	344.4	0.796	0.155	334.9
0.145	0.008	316.9	0.416	0.032	345.0	0.844	0.203	324.5
0.160	0.009	322.4	0.527	0.050	345.5	0.886	0.267	309.9
0.207	0.012	334.2	0.569	0.058	345.8			
$[N_{1122OH}][Ntf_2]$ + Water								
0.057	0.003	284.0	0.314	0.020	368.0	0.621	0.069	367.8
0.076	0.004	300.9	0.325	0.021	367.1	0.652	0.078	367.1
0.098	0.005	323.6	0.365	0.025	367.9	0.660	0.081	368.6
0.105	0.005	325.1	0.397	0.029	368.1	0.709	0.099	366.6
0.126	0.006	338.8	0.422	0.032	368.3	0.754	0.122	364.4
0.156	0.008	348.7	0.453	0.036	368.4	0.810	0.162	358.0
0.164	0.009	348.4	0.483	0.041	368.9	0.840	0.191	351.5
0.192	0.011	356.6	0.487	0.041	368.3	0.890	0.267	334.3
0.220	0.013	360.2	0.517	0.046	368.6	0.910	0.314	313.1
0.232	0.013	362.1	0.543	0.051	368.4	0.926	0.362	298.2
0.251	0.015	363.4	0.566	0.056	368.2	0.935	0.396	282.6
0.285	0.018	365.5	0.592	0.062	368.2			
$[N_{1132OH}][Ntf_2]$ + Water								
0.038	0.002	288.6	0.084	0.004	358.3	0.891	0.262	350.1
0.049	0.002	321.0	0.097	0.005	364.7	0.922	0.341	326.9
0.070	0.003	348.0	0.859	0.210	364.9	0.942	0.413	305.4
$[N_{1142OH}][Ntf_2]$ + Water								
0.025	0.001	316.9	0.889	0.252	359.2	0.929	0.355	340.6
$[N_{1152OH}][Ntf_2]$ + Water								
0.025	0.001	337.7	0.933	0.356	342.8	0.959	0.487	296.4
0.925	0.328	361.2	0.940	0.385	333.3			

The ($[N_{1112OH}][Ntf_2]$ + water + 1-octanol) mixture exhibits triple liquid–liquid immiscibility at room temperature. In order to analyze the corresponding phase diagram, a mixture containing the three components with a total weight percent composition of 38.64% (IL), 30.27% (water), and 31.08% (1-octanol) was gravimetrically prepared and allowed to phase-separate and settle for a few days. Each phase was then separated by decantation, weighted and characterized using 1H NMR to detect the ionic liquid/1-octanol ratio and coulometric Karl Fischer titration for determining the water content.

For the construction of the ternary phase diagram of the mixture ($[N_{1152OH}][Ntf_2]$ + water + 1-octanol), three samples with different total concentrations of each component were prepared gravimetrically. The analysis procedure was similar to the one used in the other studied ternary system.

Molecular Dynamics Simulations. Molecular dynamics simulations were carried out for eight different (ionic liquid plus water) or (ionic liquid plus octanol) mixtures. All simulations were performed using the DL POLY code.⁴² Water, 1-octanol, and $[N_{11n2OH}][Ntf_2]$ (where $n = 1$ and 5) ionic liquids were modeled using, respectively, the SPC model,⁴³ the OPLS-AA force field,⁴⁴ and an all-atom force field based on the CLaP force field^{45,46} specially tailored to encompass entire ionic liquid families.

For each mixture, we started from low-density initial configurations composed either of 200 ionic liquid ion pairs and 20 water or octanol molecules or 142 ion pairs and 8 water or octanol molecules. The boxes were equilibrated under isothermal–isobaric ensemble conditions for 700 ps at 303 and

350 K and 1 atm using the Nosé–Hoover thermostat and isotropic barostat with time constants of 0.5 and 2 ps, respectively. Further consecutive simulation runs of 1 ns were used to produce equilibrated systems at the studied temperature. Electrostatic interactions were treated using the Ewald summation method considering six reciprocal-space vectors, and repulsive–dispersive interactions were explicitly calculated below a cutoff distance of 1.6 nm (long-range corrections were applied assuming the system has a uniform density beyond that cutoff radius). Details concerning this type of simulation can be found elsewhere.^{45,46}

RESULTS

The LLE data of the ($[N_{11n2OH}][Ntf_2]$ ($n = 1, 2, 3, 4$, and 5) + water) and ($[N_{11n2OH}][Ntf_2]$ ($n = 1, 2, 3, 4$, and 5) + 1-octanol) binary systems are presented in Tables 2 and 3 and are depicted in Figures 1 and 2, respectively. LLE data corresponding to ($[N_{11n2OH}][Ntf_2]$ ($n = 1$ and 5) + water + 1-octanol) ternary systems at room temperature is given in Table 4.

Most binary mixtures show an UCST-type phase behavior. To obtain the critical coordinates of the different binary mixtures, the experimental data were fitted using eq 1.

Table 3. Experimental LLE Cloud-Point Temperatures of ([N_{1 1 n2OH}][Ntf₂] (IL) Plus 1-Octanol) Mixtures at Atmospheric Pressure

<i>W</i> _{IL}	<i>X</i> _{IL}	<i>T</i> /K	<i>W</i> _{IL}	<i>X</i> _{IL}	<i>T</i> /K	<i>W</i> _{IL}	<i>X</i> _{IL}	<i>T</i> /K
[N _{1 1 1 2OH}][Ntf ₂] + 1-Octanol								
0.093	0.034	348.2	0.519	0.268	371.9	0.731	0.479	371.6
0.109	0.040	353.2	0.535	0.280	371.7	0.795	0.568	370.1
0.152	0.057	359.1	0.583	0.321	372.4	0.831	0.624	368.5
0.170	0.065	361.5	0.613	0.349	371.9	0.872	0.697	364.9
0.215	0.085	363.7	0.643	0.379	372.2	0.906	0.766	360.8
0.259	0.106	365.5	0.658	0.395	371.9	0.936	0.833	345.9
0.316	0.135	368.4	0.690	0.430	372.5	0.952	0.871	332.2
0.394	0.181	370.3	0.695	0.436	371.6	0.962	0.894	323.6
0.478	0.237	371.1						
[N _{1 1 2 2OH}][Ntf ₂] + 1-Octanol								
0.055	0.019	329.9	0.420	0.191	361.0	0.774	0.529	357.1
0.120	0.043	346.7	0.468	0.223	361.5	0.826	0.608	353.6
0.193	0.072	353.8	0.501	0.247	360.9	0.868	0.683	349.4
0.240	0.093	356.8	0.578	0.310	361.3	0.870	0.687	347.1
0.290	0.118	358.7	0.636	0.363	361.0	0.898	0.743	341.3
0.333	0.140	359.6	0.672	0.401	360.6	0.914	0.776	337.7
0.368	0.160	360.1	0.726	0.464	359.4			
[N _{1 1 3 2OH}][Ntf ₂] + 1-Octanol								
0.067	0.022	316.0	0.545	0.275	338.4	0.791	0.544	332.4
0.111	0.038	324.3	0.599	0.320	338.6	0.794	0.549	331.8
0.176	0.063	330.1	0.631	0.351	338.9	0.824	0.596	327.7
0.266	0.103	334.4	0.644	0.363	338.4	0.856	0.652	323.6
0.335	0.137	338.4	0.659	0.379	338.8	0.868	0.675	320.0
0.376	0.160	338.8	0.685	0.407	338.3	0.882	0.702	318.9
0.425	0.190	338.8	0.714	0.440	337.2	0.918	0.780	310.4
0.465	0.216	338.7	0.737	0.470	336.0	0.930	0.807	303.8
0.500	0.240	338.7	0.767	0.510	334.3	0.950	0.857	279.4
[N _{1 1 4 2OH}][Ntf ₂] + 1-Octanol								
0.077	0.025	301.4	0.437	0.192	320.6	0.737	0.461	317.2
0.115	0.038	310.5	0.461	0.207	320.7	0.783	0.524	314.6
0.170	0.059	314.4	0.502	0.236	320.5	0.833	0.603	310.1
0.214	0.077	316.1	0.534	0.259	320.5	0.877	0.686	303.6
0.283	0.108	317.4	0.586	0.302	320.4	0.927	0.795	291.7
0.349	0.141	320.0	0.619	0.331	320.1	0.940	0.827	275.7
0.361	0.147	319.7	0.650	0.362	319.7			
0.418	0.180	320.4	0.691	0.405	318.6			
[N _{1 1 5 2OH}][Ntf ₂] + 1-Octanol								
0.049	0.015	272.9	0.405	0.167	299.1	0.704	0.412	296.6
0.072	0.023	282.5	0.436	0.186	299.3	0.739	0.455	296.0
0.106	0.034	287.5	0.462	0.202	300.0	0.752	0.472	295.0
0.151	0.050	295.2	0.490	0.221	299.2	0.784	0.517	293.6
0.190	0.065	297.2	0.514	0.239	299.0	0.784	0.518	294.2
0.255	0.092	297.6	0.556	0.270	299.3	0.808	0.554	290.2
0.313	0.119	298.4	0.580	0.290	299.0	0.821	0.575	290.1
0.342	0.133	298.9	0.606	0.313	298.8	0.838	0.605	288.1
0.352	0.138	298.7	0.636	0.341	298.3	0.869	0.662	282.8
0.375	0.151	298.9	0.678	0.383	297.3	0.916	0.763	270.5

$$T = \begin{cases} T_c - \left[T_c \times \left(\frac{|w - w_c|}{A_{\text{left}}} \right)^{1/\beta} \right], & w \leq w_c \\ T_c - \left[T_c \times \left(\frac{|w - w_c|}{A_{\text{right}}} \right)^{1/\beta} \right], & w \geq w_c \end{cases} \quad (1)$$

The fitting parameters obtained are reported in Table 5 for each type of system. The fitted values are also reported in

Tables 2 and 3 and represented in Figures 1 and 2. The maximum difference between the experimental temperature values and the corresponding fitting data is 2 K.

The ionic liquid plus water systems show almost symmetrical phase diagrams if the composition of the system is given in mass fraction; i.e., at a given temperature the mutual solubilities of the two compounds (IL in water and water in IL) are similar if expressed in mass percentage. Due to the large difference between the molar masses of the ionic liquids and that of water,

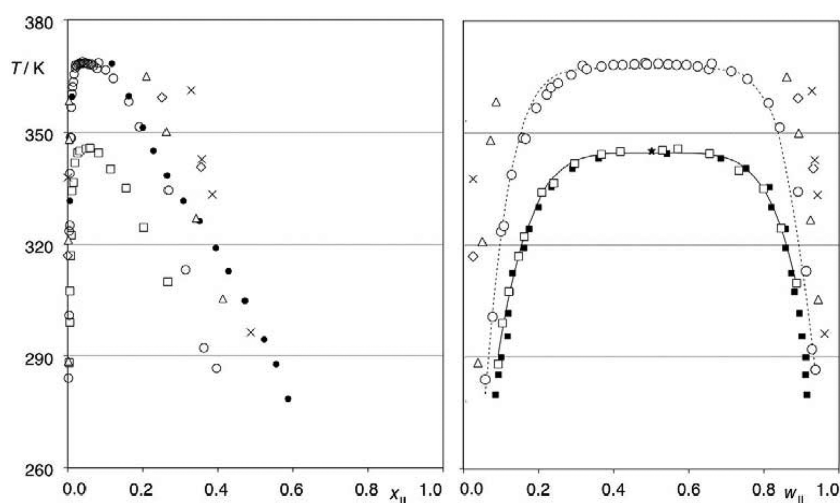


Figure 1. Temperature–composition phase diagrams showing the LLE behavior of binary mixtures of $[N_{1.1n.2OH}][Ntf_2]$ (IL) with water at atmospheric pressure. Compositions in the left panel are in mole fraction; those on the right are in weight fraction. (\square) C1, $[N_{1.1.2OH}][Ntf_2]$; (\circ) C2, $[N_{1.1.2.2OH}][Ntf_2]$; (\triangle) C3, $[N_{1.1.3.2OH}][Ntf_2]$; (\diamond) C4, $[N_{1.1.4.2OH}][Ntf_2]$; (\times) C5, $[N_{1.1.5.2OH}][Ntf_2]$; (\bullet) ref 38; (\blacksquare) ref 37. The solid and dashed lines on the right panel represent the fittings to the C1 and C2 data (eq 1).

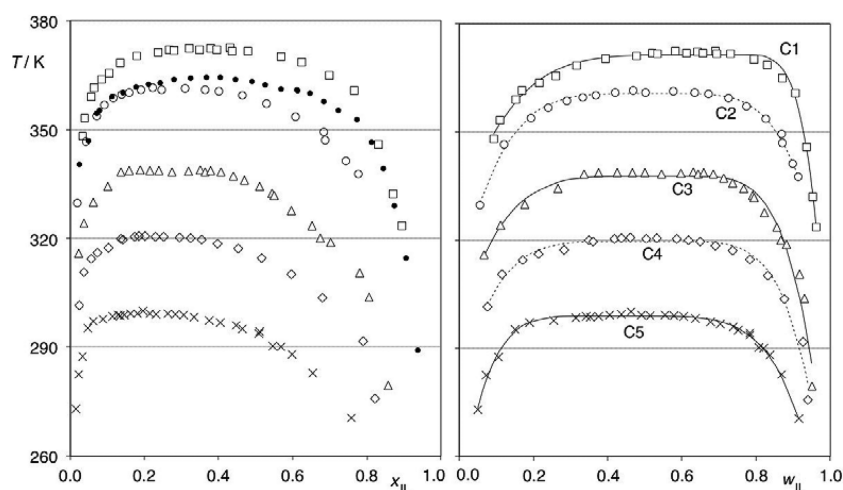


Figure 2. Temperature–composition phase diagrams showing the LLE behavior of binary mixtures of $[N_{1.1n.2OH}][Ntf_2]$ (IL) with 1-octanol at atmospheric pressure. Compositions in the left panel are in mole fraction; those on the right are in weight fraction. (\square) C1, $[N_{1.1.2OH}][Ntf_2]$; (\circ) C2, $[N_{1.1.2.2OH}][Ntf_2]$; (\triangle) C3, $[N_{1.1.3.2OH}][Ntf_2]$; (\diamond) C4, $[N_{1.1.4.2OH}][Ntf_2]$; (\times) C5, $[N_{1.1.5.2OH}][Ntf_2]$; (\bullet) ref 38. The solid and dashed lines on the right panel represent the fittings obtained using eq 1.

such symmetry is not preserved if the diagrams are represented as a function of mole fraction.

UCSTs could only be determined for the systems with $[N_{1.1.1.2OH}][Ntf_2]$ and $[N_{1.1.2.2OH}][Ntf_2]$ and the fitted results (Table 5) show that whereas the critical mass fraction is similar for both ionic liquids ($w_{LCST} = 0.5$), the critical temperatures differ by 22.9 K, with $[N_{1.1.1.2OH}][Ntf_2]$ showing a higher miscibility window than $[N_{1.1.2.2OH}][Ntf_2]$. Even with only partial data for the remaining three $[N_{1.1n.2OH}][Ntf_2]$ aqueous systems, the results clearly show that the ionic liquid–water mutual solubilities tend to decrease with the increase in the alkyl chain in the cholinium cation.

The results compare favorably with other data previously reported in the literature.^{37,38} In the case of the $([N_{1.1.1.2OH}][Ntf_2] + H_2O)$ system, a direct quantitative analysis is hard to perform since Nockemann et al.³⁷ chose to report their data only in graphical form. Nevertheless, theirs and the present data match within the estimated temperature and composition uncertainties (Figure 1). In the case of the $([N_{1.1.2.2OH}][Ntf_2] +$

H_2O) system, the few data points reported by Domanska et al.³⁸ in the LLE region also agree with the present results, although no comparisons are possible in the region near the critical composition of the UCST (Figure 1). For mixtures with higher ionic liquid mole fraction, our demixing temperatures are lower than those reported in ref 38. The discrepancy can be attributed to different levels of purity or water content in the ionic liquid samples or to a different methodology used in the VLE measurements—instead of determining the demixing temperature of a given mixture upon cooling (appearance of turbidity), those authors chose to ascertain the mixing temperature upon heating (turbidity disappearance). Their method is specially suited to SLE determinations (crystal disappearance) but harder to implement for LLE conditions.

In the case of the $([N_{1.1n.2OH}][Ntf_2] + 1\text{-octanol})$ systems, the envelopes of the LLE region are not as symmetrical as in the case of the aqueous mixtures: if the values are reported in mass percentage, the solubility of the ILs in 1-octanol is lower than that of 1-octanol in the ILs. An increase in the alkyl chain

Table 4. Experimental LLE Data of $([N_{1\ 1\ n\ 2OH}][Ntf_2] \text{ (IL, } n = 1 \text{ or } 5) + \text{Water} + 1\text{-Octanol})$ Ternary Mixtures at 300 K and Atmospheric Pressure

phase	w_{IL}	w_{water}	$w_{octanol}$
$([N_{1\ 1\ 2OH}][Ntf_2] + \text{Water} + 1\text{-Octanol})$			
global	0.38642	0.30273	0.31083
IL-rich	0.86428	0.10613	0.02957
water-rich	0.13776	0.85247	0.00976
octanol-rich	0.13927	0.08983	0.77088
$([N_{1\ 1\ 5OH}][Ntf_2] + \text{Water} + 1\text{-Octanol})$			
global (i)	0.17024	0.33007	0.49968
water-rich (i)	0.10172	0.89000	0.00827
water-poor (i)	0.19383	0.06066	0.74550
global (ii)	0.43918	0.05334	0.50747
water-rich (ii)	0.33814	0.33176	0.33008
water-poor (ii)	0.11800	0.87000	0.01199
global (iii)	0.69192	0.04547	0.26259
water-rich (iii)	0.49992	0.32987	0.17019
water-poor (iii)	0.11382	0.88000	0.00617

Table 5. Parameters of the Scaling-Type Equation (Eq 1) for Binary Mixtures of $[N_{1\ 1\ n\ 2OH}][Ntf_2]$ with Water or 1-Octanol at Atmospheric Pressure

cation	A_{left}	A_{right}	β	T_c	w_c
$[N_{1\ 1\ n\ 2OH}][Ntf_2] + \text{Water}$					
$[N_{1112OH}]^+$	0.612	0.612 ^a	0.209	344.7	0.51
$[N_{1122OH}]^+$	0.557	0.557 ^a	0.159	367.6	0.50
$[N_{1\ 1\ n\ 2OH}][Ntf_2] + 1\text{-Octanol}$					
$[N_{1112OH}]^+$	1.073	0.356	0.189	371.3	0.72
$[N_{1122OH}]^+$	0.818	0.691	0.217	360.7	0.53
$[N_{1132OH}]^+$	0.855	0.570	0.202	337.9	0.56
$[N_{1142OH}]^+$	0.753	0.628	0.187	319.7	0.51
$[N_{1152OH}]^+$	0.569	0.783	0.185	298.9	0.41

^aConstrained to yield a symmetrical curve.

length of the cation increases the miscibility region for these mixtures—the UCSTs drop from 371 K for the $([N_{1\ 1\ 2OH}][Ntf_2] + 1\text{-octanol})$ system to 299 K for the $([N_{1\ 1\ 5OH}][Ntf_2] + 1\text{-octanol})$ system. The estimated critical mass fractions of the binary systems, w_{UCST} , also tend to decrease, from a value of 0.7 for $([N_{1\ 1\ 2OH}][Ntf_2] + 1\text{-octanol})$ to around 0.4 for $([N_{1\ 1\ 5OH}][Ntf_2] + 1\text{-octanol})$.

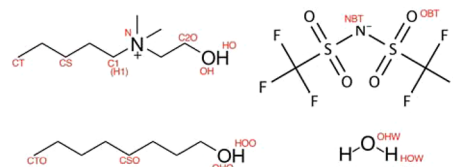
Comparison with the Domanska et al.³⁸ results for the $([N_{1\ 1\ 2OH}][Ntf_2] + 1\text{-octanol})$ system show good agreement at low ionic liquid concentration but progressively larger deviations for IL-rich mixtures (demixing temperature differences can be as high as 10 K for compositions on the IL-rich side of the diagram). Nevertheless, the estimation of UCSTs for this particular binary mixture from the two distinct sets of data yield comparable results: 364.3 K (ref 38) versus 360.7 K (this work). As before, the observed differences can be linked to the purity of the ionic liquid samples or the methodology used in the LLE determinations.

DISCUSSION

The solubility of ionic liquids in molecular solvents and vice versa depends on the interactions between the components of the mixture. The experimental data shows that an increase in the alkyl chain length of the cation has a marked influence in the UCST of the systems, with water and 1-octanol yielding opposite trends: in the former case, an increase in the alkyl

chain length of the cation reduces the 1-phase region of the phase diagram; in the latter case, miscibility is enhanced by the increase in the chain length of the ionic liquid. These results per se are not unexpected given the hydrophilic/hydrophobic character of the two molecular solvents—which are in fact used together to determine the nature of different solutes via the determination of octanol–water partition coefficients—and the progressively more hydrophobic nature of ionic liquids as the nonpolar moieties (alkyl chains) of their ions are increased. What is remarkable in the present data is that (i) the liquid nature of the three compounds (water, 1-octanol, and ILs) leads to phase equilibria that are not disturbed by the precipitation of any solid phases in the studied temperature range; (ii) the phase behavior can be quantified in both directions by the measurement of the UCSTs of the corresponding liquid–liquid equilibria; and (iii) the mutual solubilities (given in mass or volume fraction) in the IL–water or in the IL–octanol binary systems are quite similar, yielding quite symmetrical phase diagrams. These three points will be considered in the following discussion.

As mentioned at the beginning of the previous paragraph, the interpretation at a molecular level of the phase behavior of mixtures implies the knowledge of the interactions between their components. If some of the intervening phases are solid, one expects that the stability of the corresponding crystals (dominated by specific interactions and packing constraints) will play a significant role in the determination of the overall equilibrium. From the interactions point of view, this fact adds extra complexity to systems that are already quite complex in the liquid phase (hydrogen bonding in water and 1-octanol; ionic versus dispersive forces in ionic liquids). In the case of octanol–water partition experiments with ionic or molecular compounds that are solid in the temperature ranges of liquid water and liquid 1-octanol (a working range at atmospheric pressure between $280 < T/K < 380$) such unwanted outcome (added complexity caused by the precipitation of the solute) is unavoidable. However, ionic liquids with melting temperatures around or below room temperature yield IL–water and IL–octanol binary systems that are dominated by LLE and even the possibility of ternary systems with triple liquid–liquid immiscibility (see further discussion below). This means that the interpretation of the fluid phase behavior of the mixtures in terms of interactions at a molecular level can be performed in a more straightforward way using for instance molecular modeling and simulation tools. In the present work, we have used molecular dynamics results (cf. Scheme 1) obtained from the study of selected binary systems (the four combinations of $[N_{1\ 1\ 2OH}][Ntf_2]$ or $[N_{1\ 1\ 5OH}][Ntf_2]$ + water or 1-octanol) under two temperatures inside the studied temperature range (298 and 350 K). As mentioned in the Introduction, $[Ntf_2]$ -

Scheme 1. Nomenclature Used in the Molecular Dynamics Simulations and Discussion To Define the Different Interaction Centers in the Two Ions of the $[N_{1\ 1\ n\ 2OH}][Ntf_2]$ Ionic Liquids (top) and the Two Molecular Solvents (bottom)

based ionic liquids have the advantage of exhibiting lower melting points relative to other similar ionic liquids based on other anions (a relevant issue considering what was just said in the previous paragraph). Another characteristic of $[\text{Ntf}_2]$ -based ionic liquids is that they are generally dubbed as “hydrophobic”; i.e., either they are only partially immiscible with water in their entire working temperature range or they exhibit UCSTs well above room temperature. In this context the studied $[\text{N}_{1112}\text{OH}][\text{Ntf}_2]$ ionic liquids are in fact different from the more common ones based on the 1-alkyl-3-methylimidazolium cation ($[\text{C}_n\text{C}_1\text{im}][\text{Ntf}_2]$): whereas aqueous mixtures of $[\text{C}_n\text{C}_1\text{im}][\text{Ntf}_2]$ are generally dominated by LLE over the entire or most of the temperature range (no measurable UCSTs), aqueous mixtures of $[\text{N}_{1112}\text{OH}][\text{Ntf}_2]$ and $[\text{N}_{1112}\text{OH}][\text{Ntf}_2]$ exhibit UCSTs at 345 and 367 K, respectively. Moreover the imidazolium-based systems also exhibit a pronounced asymmetry in terms of the mutual solubilities of the two compounds in the aqueous mixtures—the IL can dissolve some water molecules but almost no ionic liquid is dissolved in water—a point that is not true for the cholinium-based systems and that will be further discussed below.

The difference between the $[\text{N}_{1112}\text{OH}][\text{Ntf}_2]$ and $[\text{C}_n\text{C}_1\text{im}][\text{Ntf}_2]$ aqueous systems can be inferred from the radial distribution functions obtained from simulations of a few water molecules dissolved in the choline-based ionic liquids (Figures 3 and 4). Previous works⁴⁷ have shown that the solubility of water in ionic liquids is controlled by the different affinity of the water molecule toward the anion or cation of the ionic liquid. In general the stronger the interactions the more

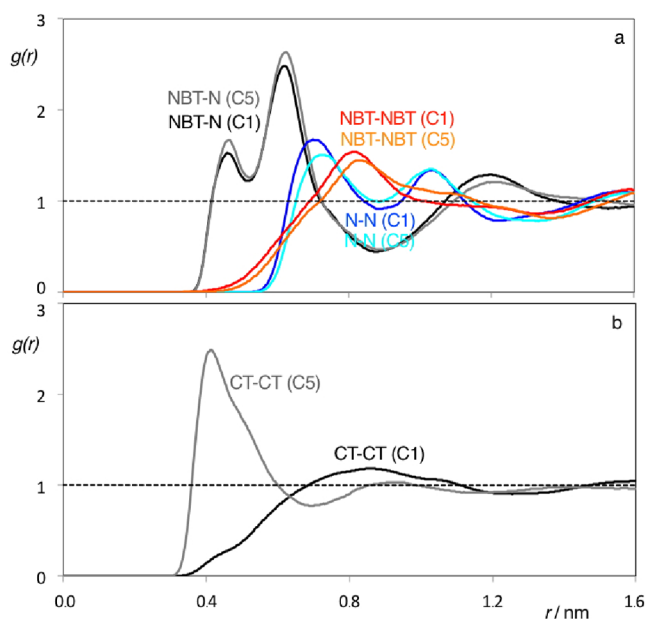


Figure 3. Radial distribution functions (RDFs, $g(r)$) for selected interaction centers of $[\text{N}_{1112}\text{OH}][\text{Ntf}_2]$ (C1) and $[\text{N}_{1152}\text{OH}][\text{Ntf}_2]$ (C5) in mixtures containing 1-octanol at 350 K (cf. Scheme 1): (a) the highly structured polar network of both ionic liquids can be appreciated given the out-of-phase character of the RDFs corresponding to anion–cation interactions (black/gray) versus cation–cation (blue/cyan) or anion–anion (red/orange) interactions; (b) the completely different nanosegregated nature of $[\text{N}_{1112}\text{OH}][\text{Ntf}_2]$ and $[\text{N}_{1152}\text{OH}][\text{Ntf}_2]$ is shown by the absence (black) and presence (gray) of nonpolar domains in the ionic liquid.

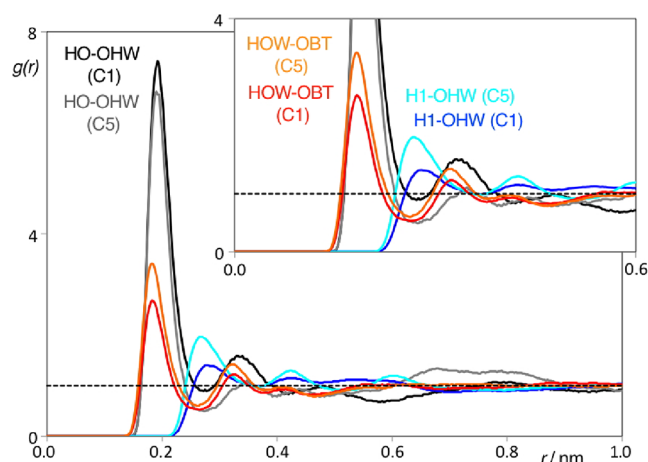


Figure 4. Radial distribution functions (RDFs, $g(r)$) for selected interaction centers of $[\text{N}_{1112}\text{OH}][\text{Ntf}_2]$ (C1), $[\text{N}_{1152}\text{OH}][\text{Ntf}_2]$ (C5) in mixtures with water molecules at 350 K (cf. Scheme 1). The six RDFs depict the interactions between the water molecules and the different interaction centers in the two ionic liquids: the presence of strong interactions between the OH group of the cation and water is indicated by the conspicuous black/gray RDFs; the inset shows in more detail the RDFs between water and the charged parts of the anion (red/orange) and cation (blue/cyan).

hydrophilic the ionic liquid but a tendency to bind selectively to just one type of ion can have a detrimental effect. This is the case of $[\text{C}_n\text{C}_1\text{im}][\text{Ntf}_2]$ ionic liquids where water strongly competes with the cation for strong interactions with the $[\text{Ntf}_2]^-$ anion. At a certain point the cations do not allow the anions to be solvated by more water molecules since that would compromise local electroneutrality conditions and liquid–liquid demixing occurs (an ionic liquid-rich phase “saturated” in water separates from a second phase that is almost pure water). In the case of $[\text{N}_{1112}\text{OH}][\text{Ntf}_2]$ ionic liquids the cation has an extra interaction center that can promote its binding to the water molecules (the hydroxyl group at the end of its ethyl group of the cholinium-based cation is able to form a hydrogen-like bond or establish dipole–dipole interactions with the water molecules, Figure 4). This means that the interaction of the water molecules with the two ions is more balanced, which allows for a better dissolution of water molecules among the ionic network of the ionic liquid (IL-rich mixtures) and the solvation of ionic aggregates in the midst of water (water-rich mixtures). These two sorts of enhanced interaction cause lower UCSTs and a more symmetrical phase diagram in terms of mass or volume fraction of the mixture. Due to the large difference in molar mass and molar volume between the water molecules and ionic liquid ions the solvation/interaction ratio between the two components of the mixture is very different from unity (several water molecules can solvate one ion pair; several ionic pairs cannot interact with a single water molecule). This means that the phase diagrams depicted in terms of mole fraction will always show critical compositions of the UCSTs skewed toward water-rich mixtures (Figure 1b).

It must be stressed at this point that the hydrogen-bond-type interactions between the hydroxyl group of the cholinium-based cations and the water molecules help to promote the miscibility and lower the otherwise very high UCSTs (like in the case of imidazolium-based ILs) but are not crucial in determining the existence of the UCSTs or their dependence with the alkyl chain length of the rest of the cholinium-based

cations. In fact, if hydrogen bonding between water and the OH group of the cholinium-based cations were dominant at around room temperature, it would become less so at higher temperatures, which would mean that as temperature went up the systems would tend to remain (or become) demixed (a entropically driven effect that generally promotes LCST and not UCSTs). The demixing at lower temperatures in the aqueous $[N_{1112OH}][Ntf_2]$ is defined by the above-mentioned effect of segregation of water molecules by the ionic network in order to preserve the local neutrality conditions of the liquid media and by the hydrophobic effect caused by the presence of more or less important nonpolar residues (alkyl chains) attached to the cation. The latter effect explains the dependence of the UCSTs with the size of the alkyl residues.

In the $([N_{1112OH}][Ntf_2] + 1\text{-octanol})$ binary systems, the presence of UCSTs at different temperatures is also conspicuous but the effect is the opposite of that found for the aqueous solutions. In this case, the dispersion interactions between the alkyl chains of the cation and that of the 1-octanol molecule are responsible for the position and dependence of the UCSTs along the IL homologous series. This can be directly checked if one takes into account the radial distribution functions between the terminal carbon atoms, CTO and CT, of the octyl chain of the 1-octanol molecule and the alkyl chain of the $[N_{1112OH}]$ cation, respectively (Figure 5). The CTO-CT RDFs of the $([N_{1112OH}][Ntf_2] + 1\text{-octanol})$ and $([N_{1152OH}][Ntf_2] + 1\text{-octanol})$ systems show that the octyl residue of the 1-octanol molecule is accommodated inside an alkane-like

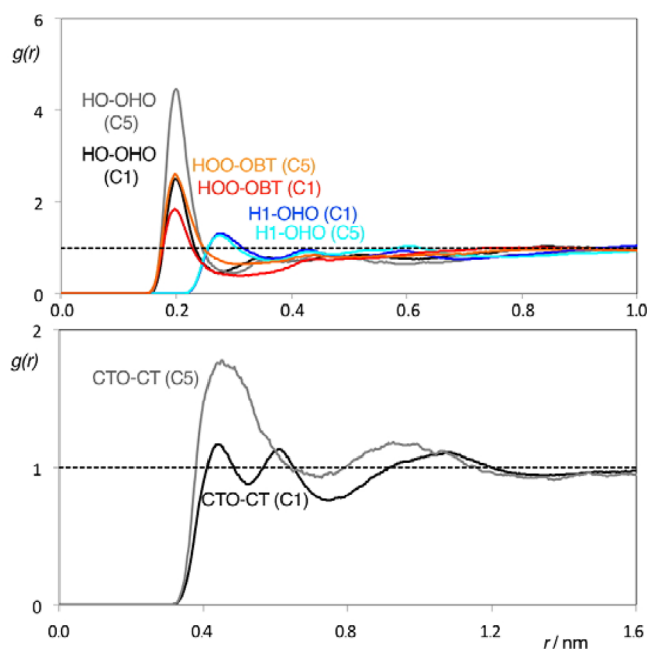


Figure 5. Radial distribution functions (RDFs, $g(r)$) for selected interaction centers of $[N_{1112OH}][Ntf_2]$ (C1), $[N_{1152OH}][Ntf_2]$ (C5), and 1-octanol in mixtures at 350 K (cf. Scheme 1). (a) The three sets of RDFs depict the interactions between the hydroxyl group of 1-octanol and the different interaction centers of the ionic liquid. These are subdued versions of the RDFs presented in Figure 4. The more intense C5 RDFs are caused by a normalization effect due to the “dilution” of the polar network in a ionic liquid with large nonpolar domains. (b) The placement of the alkyl chain of the octanol molecule inside the nonpolar domains of the C5 (broad gray peak) ionic liquid is clearly seen by comparison with the corresponding RDF for C1 (black), where no such peak is observed.

domain in the latter case but remains near the polar network of the IL (that occupies most of the available volume) in the former situation. The lack of segregated nonpolar domains in the $[N_{1112OH}][Ntf_2]$ ionic liquid causes the high UCST of the $([N_{1112OH}][Ntf_2] + 1\text{-octanol})$ system.

It is also interesting to note the role of the hydroxyl group of the octanol molecule in the fluid phase behavior of the mixtures under discussion. First, one can think that the hydrogen-bonding and dipole–dipole interactions that are present in the aqueous mixtures should also be present (to a limited extent) in the octanol-based mixtures (after all the hydroxyl group of an alcohol can be regarded as “half-water”). Indeed, the RDFs show that there are always interactions between the OH group of the choline-based cations and the OH group of octanol (Figure 5). The RDFs also show that in fact such interactions remain active even when the rest of the octyl chain plunges further into the larger nonpolar domains of ILs with long alkyl chains.

The regular behavior of the solubility trends of the aqueous and octanol mixtures along the homologous choline-based IL series and the relevance of the octanol–water partition coefficients in many chemical and biological areas led us to prepare and analyze two ternary 1-octanol–water–IL mixtures.

First, we chose the $([N_{1112OH}][Ntf_2] + 1\text{-octanol} + \text{water})$ ternary system since the corresponding binary mixtures present large mutual immiscibility windows around room temperature. In fact, the system presents triple liquid–liquid immiscibility and analyses of the three phases at equilibrium defined the schematic ternary phase diagram presented in Figure 6. In this

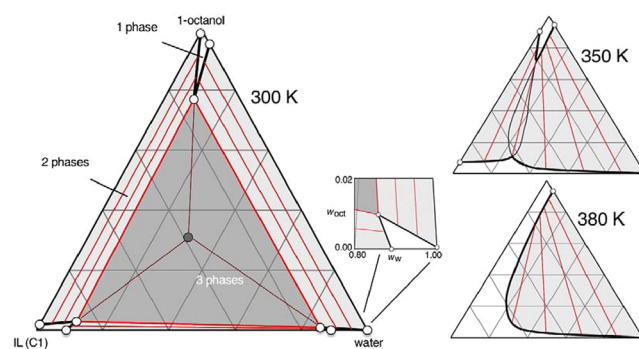


Figure 6. Triangular phase diagrams of the ternary system $([N_{1112OH}][Ntf_2]$ (IL C1) + water + 1-octanol) at three different temperatures. The circles represent experimental LLE data obtained at 300 K in three binary and one ternary mixtures (the gray circle denotes the total composition of the latter). Tie lines in the two-phase regions are indicated as red lines; those in the triple liquid immiscibility region are depicted as brown segments. The inset shows a magnified view of the tip of the diagram corresponding to the water-rich one-phase region.

case the system is definable not just by the usual octanol–water partition coefficient of the ionic liquid in the two saturated water-rich and octanol-rich solutions but also by the fact that there is a third ionic liquid-rich liquid phase—partition coefficients of water in the IL-rich and octanol-rich phases and of 1-octanol in the IL-rich and water-rich phases can also be established. The points obtained in the triangular diagram at 300 K show that (i) the wedge shape of the one-phase regions at the upper tip of the triangular diagram indicates that there is some sort of cosolvency effect for octanol-rich solutions, specially when water is added to a IL-saturated octanol

solution; (ii) the edges of the one-phase regions and the placement of the three-phase region also suggest that $[N_{1112OH}][Ntf_2]$ + water immiscibility is more limited than $[N_{1112OH}][Ntf_2]$ + octanol or water + octanol miscibilities; (iii) such fact can be confirmed by plotting triangular diagrams at higher temperatures based on the mutual solubilities of the three components in the corresponding binary mixtures: at 350 K $[N_{1112OH}][Ntf_2]$ and water are completely miscible and the three-phase region is replaced by an immiscibility corridor joining two of the sides of the triangular diagram. At 380 K $[N_{1112OH}][Ntf_2]$ and 1-octanol are also miscible and the corridor is replaced by the usual liquid–liquid immiscibility window (right side of the diagram) that shows that at that temperature $[N_{1112OH}][Ntf_2]$ is capable of promoting some degree of miscibility between 1-octanol and water.

In the case of the $([N_{1152OH}][Ntf_2]$ + 1-octanol + water) ternary system we have considered three different mixtures at 300 K (Table 5). The corresponding triangular diagram (Figure 7) does not show triple liquid immiscibility. Instead, it exhibits

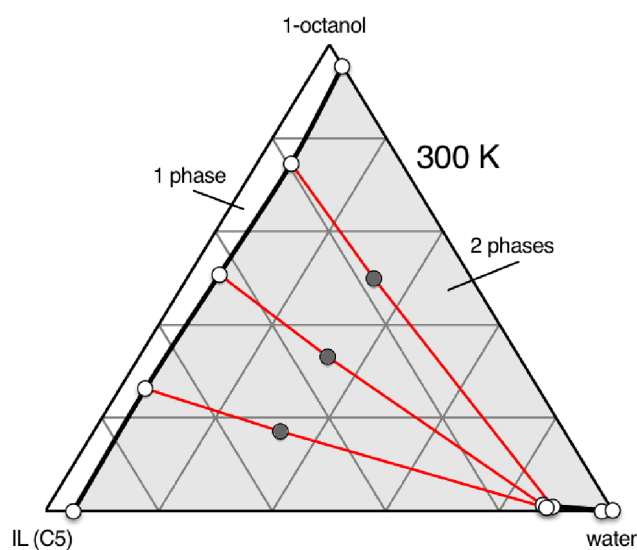


Figure 7. Triangular phase diagram of the ternary system $([N_{1152OH}][Ntf_2]$ (IL (C5)) + water + 1-octanol) at 300 K. The circles represent experimental LLE data obtained in the corresponding binary and ternary mixtures (the gray circles correspond to the total composition three different ternary mixtures). Tie lines in the two-phase regions are represented as red lines.

an immiscibility corridor with morphology similar to the one present in Figure 6b. The main difference between the two figures is the orientation of the corridors: whereas $[N_{1112OH}][Ntf_2]$ is miscible with 1-octanol and immiscible with water at 300 K (oblique corridor), the case is reversed for $[N_{1112OH}][Ntf_2]$ at 350 K (horizontal corridor). Moreover, considering the data obtained for the corresponding binary systems at different temperatures, the composition–temperature triangular prism should be more regular for the ternary systems containing $[N_{1152OH}][Ntf_2]$ (the immiscibility corridor will remain at higher temperatures) than for the systems containing $[N_{1112OH}][Ntf_2]$ (where sections of the prism evolve from a triple liquid immiscibility situation at 300 K to a immiscibility corridor at 350 K and a immiscibility window at 380 K, Figure 6).

CONCLUSIONS

The liquid–liquid equilibria of mixtures of cholinium-based ionic liquids (*N*-alkyl-*N,N*-dimethylhydroxyethylammonium bis(trifluoromethane)sulfonylimide, $[N_{11n2OH}][Ntf_2]$, $n = 1, 2, 3, 4$, and 5) plus water or 1-octanol show that the behavior of this particular ionic liquid homologous family toward each of the molecular solvents is quite diverse and can be fine-tuned by taking into account the length of the alkyl side chain present in the cholinium-derived cation. Two other interrelated factors also play an important role in the definition of the various LLE envelopes (windows/corridors/triple immiscibility): the presence of hydroxyl groups in the cation and the effect of temperature.

The existence of measurable upper critical solution temperatures for most of the studied systems and the fact that LLE trends along the homologous IL series are reversed when either aqueous or 1-octanol binary systems are considered allowed us to rationalize at a molecular level the systematic behavior shifts for this particular IL family. New studies where the natures of both the molecular solvent and the cholinium-based ionic liquid are further modified are currently under way.

ASSOCIATED CONTENT

Supporting Information

NMR analyses of the ILs synthesized in this work. This material is available free of charge via the Internet at <http://pubs.acs.org>.

AUTHOR INFORMATION

Corresponding Author

*E-mail: jnlopes@ist.utl.pt (J.N.C.L.); jmesp@itqb.unl.pt (J.M.S.S.E.).

Notes

The authors declare no competing financial interest.

ACKNOWLEDGMENTS

Financial support provided by Fundação para a Ciência e Tecnologia (FCT) through projects PTDC/QUI/71331/2006, PTDC/QUI-QUI/101794/2008, PTDC/EQU-EQU/102949/2008, PTDC/CTM-NAN/121274/2010, PEst-OE/QUI/UI0100/2011, and PEst-OE/EQB/LA0004/2011. The National NMR Network (REDE/1517/RMN/2005) was supported by POCI 2010 and Fundação para a Ciência e a Tecnologia. J.M.S.S.E. and I.M.M. acknowledge FCT for a contract under Programa Ciência 2007. K.S. acknowledges the grant SFRH/BPD/38339/2007.

REFERENCES

- (1) Blusztajn, J. K. *Science* **1998**, *281*, 794–795.
- (2) Jones, J. P., III; Meck, W. H.; Williams, C. L.; Wilson, W. A.; Swartzwelder, H. S. *Dev. Brain Res.* **1999**, *118*, 159–167.
- (3) Meck, W. H.; Williams, C. L. *Dev. Brain Res.* **1999**, *118*, 51–59.
- (4) Gathergood, N.; Garcia, M. T.; Scammells, P. J. *Green Chem.* **2004**, *6*, 166–175.
- (5) Rebelo, L. P. N.; Canongia Lopes, J. N.; Esperança, J. M. S. S.; Filipe, E. J. *Phys. Chem. B* **2005**, *109*, 6040–6043.
- (6) Earle, M. J.; Esperança, J. M. S. S.; Gilea, M. A.; Lopes, J. N. C.; Rebelo, L. P. N.; Magee, J. W.; Seddon, K. R.; Widegren, J. A. *Nature* **2006**, *439*, 831–834.
- (7) Smiglak, M.; Reichert, W. M.; Holbrey, J. D.; Wilkes, J. S.; Sun, L. Y.; Thrasher, J. S.; Kirichenko, K.; Singh, S.; Katritzky, A. R.; Rogers, R. D. *Chem. Commun.* **2006**, 2554–2556.

- (8) Esperança, J. M. S. S.; Canongia Lopes, J. N.; Tariq, M.; Santos, L. M. N. B. F.; Magee, J. W.; Rebelo, L. P. N. *J. Chem. Eng. Data* **2010**, *55*, 3–12.
- (9) Domanska, U. *Thermochim. Acta* **2006**, *448*, 19–30.
- (10) Stolte, S.; Arning, J.; Bottin-Weber, U.; Matzke, M.; Stock, F.; Thiele, K.; Uerdingen, M.; Jastorff, B.; Ranke, J. *Green Chem.* **2006**, *8*, 621–629.
- (11) Stolte, S.; Arning, J.; Bottin-Weber, U.; Müller, A.; Pitner, W. R.; Welz-Biermann, U.; Jastorff, B.; Ranke, J. *Green Chem.* **2007**, *9*, 760–767.
- (12) Nockemann, P.; Thijs, B.; Driesen, K.; Janssen, C. R.; Hecke, K. V.; Meervelt, L. V.; Kossmann, S.; Kirchner, B.; Binnemans, K. *J. Phys. Chem. B* **2007**, *111*, 5254–5263.
- (13) Wang, X.; Ohlin, C. A.; Lu, Q.; Fei, Z.; Hub, J.; Dyson, P. J. *Green Chem.* **2007**, *9*, 1191–1197.
- (14) Yu, Y.; Lu, X.; Zhou, Q.; Dong, K.; Yao, H.; Zhang, S. *Chem.—Eur. J.* **2008**, *14*, 11174–11182.
- (15) Marija Petkovic, M.; Ferguson, J. L.; Gunaratne, H. K. N.; Ferreira, R.; Leitão, M. C.; Seddon, K. R.; Rebelo, L. P. N.; Pereira, C. P. *Green Chem.* **2010**, *12*, 643–649.
- (16) Weaver, K. D.; Kim, H. J.; Sun, J.; MacFarlane, D. R.; Elliott, G. D. *Green Chem.* **2010**, *12*, 507–513.
- (17) Abelló, S.; Medina, F.; Rodríguez, X.; Cesteros, Y.; Salagre, P.; Sueiras, J. E.; Tichit, D.; Coq, B. *Chem. Commun.* **2004**, 1096–1097.
- (18) Abbott, A. P.; Bell, T. J.; Handa, S.; Stoddart, B. *Green Chem.* **2005**, *7*, 705–707.
- (19) Hu, S.; Jiang, T.; Zhang, Z.; Zhu, A.; Han, B.; Song, J.; Xie, Y.; Li, W. *Tetrahedron Lett.* **2007**, *48*, 5613–5617.
- (20) Moriel, P.; García-Suárez, E. J.; Martínez, M.; García, A. B.; Montes-Morán, M. A.; Calvino-Casilda, V.; Bañares, M. A. *Tetrahedron Lett.* **2010**, *51*, 4877–4881.
- (21) Gorke, J.; Srien, F.; Kazlauskas, R. *Biotechnol. Bioprocess Eng.* **2010**, *15*, 40–53.
- (22) Avalos, M.; Babiano, R.; Cintas, P.; Jimenez, J. L.; Palacios, J. C. *Angew. Chem., Int. Ed.* **2006**, *45*, 3904–3908.
- (23) Abbott, A. P.; Frisch, G.; Hartley, J.; Ryder, K. S. *Green Chem.* **2011**, *13*, 471–481.
- (24) Vijayaraghavan, R.; Thompson, B. C.; MacFarlane, D. R.; Kumar, R.; Surianarayanan, M.; Aishwary, S.; Sehgal, P. K. *Chem. Commun.* **2010**, *46*, 294–296.
- (25) Fujita, K.; MacFarlane, D. R.; Forsyth, M.; Yoshizawa-Fujita, M.; Murata, K.; Nakamura, N.; Ohno, H. *Biomacromolecules* **2007**, *8*, 2080–2086.
- (26) Crosthwaite, J. M.; Aki, S. N. V. K.; Maginn, E. J.; Brennecke, J. F. *J. Phys. Chem. B* **2004**, *108*, 5113–5119.
- (27) Domanska, U.; Marciniak, A. *Fluid Phase Equilib.* **2007**, *260*, 9–18.
- (28) Lachwa, J.; Szydlowski, J.; Najdanovic-Visak, V.; Rebelo, L. P. N.; Seddon, K. R.; Ponte, M. N.; Esperança, J. M. S. S.; Guedes, H. J. R. *J. Am. Chem. Soc.* **2005**, *127*, 6542–6543.
- (29) Lachwa, J.; Szydlowski, J.; Makowska, A.; Seddon, K. R.; Esperança, J. M. S. S.; Guedes, H. J. R.; Rebelo, L. P. N. *Green Chem.* **2006**, *8*, 262–267.
- (30) Deive, F. J.; Rodriguez, A.; Pereiro, A. B.; Shimizu, K.; Forte, P. A. S.; Romão, C. C.; Lopes, J. N. C.; Esperança, J. M. S. S.; Rebelo, L. P. N. *J. Phys. Chem. B* **2010**, *114*, 7329–7337.
- (31) Pereiro, A. B.; Araujo, J. M. M.; Esperança, J. M. S. S.; Marrucho, I. M.; Rebelo, L. P. N. *J. Chem. Thermodyn.* **2012**, *46*, 2–28.
- (32) Lachwa, J.; Morgado, P.; Esperança, J. M. S. S.; Guedes, H. J. R.; Lopes, J. N. C.; Rebelo, L. P. N. *J. Chem. Eng. Data* **2006**, *51*, 2215–2221.
- (33) Crosthwaite, J. M.; Aki, S. N. V. K.; Maginn, E. J.; Brennecke, J. F. *Fluid Phase Equilib.* **2005**, *228*, 303–309.
- (34) Vale, V. R.; Will, S.; Schroer, W.; Rathke, B. *ChemPhysChem* **2012**, *13*, 1860–1867.
- (35) Domanska, U.; Rekawek, A.; Marciniak, A. *J. Chem. Eng. Data* **2008**, *53*, 1126–1132.
- (36) Freire, M. G.; Carvalho, P. J.; Gardas, R. L.; Marrucho, I. M.; Santos, L. M. N. B. F.; Coutinho, J. A. P. *J. Phys. Chem. B* **2008**, *112*, 1604–1610.
- (37) Nockemann, P.; Binnemans, K.; Thijs, B.; Parac-Vogt, T. N.; Merz, K.; Mudring, A. V.; Menon, P. C.; Rajesh, R. N.; Cordoyiannis, G.; Thoen, J.; Leys, J.; Glorieux, C. *J. Phys. Chem. B* **2009**, *113*, 1429–1437.
- (38) Domańska, U.; Marciniak, A.; Krolikowski, M. *J. Phys. Chem. B* **2008**, *112*, 1218–1225.
- (39) Domańska, U.; Pobudkowska, A.; Krolikowski, M. *Fluid Phase Equilib.* **2007**, *259*, 173–179.
- (40) Domańska, U.; Bogel-Lukasik, R. *J. Phys. Chem. B* **2005**, *109*, 12124–12132.
- (41) Costa, A. J. L.; Soromenho, M. R. C.; Shimizu, K.; Marrucho, I. M.; Esperança, J. M. S. S.; Lopes, J. N. C.; Rebelo, L. P. N. *ChemPhysChem* **2012**, *13*, 1902–1909.
- (42) Smith, W.; Forester, T. R.; Todorov, I. T. *The DL-POLY 2 User Manual, Version 2.20*; STFC Daresbury Laboratory: Warrington, UK, 2009.
- (43) Praprotnik, M.; Janežič, D.; Mavri, J. *J. Phys. Chem. A* **2004**, *108*, 11056–11062.
- (44) Jorgensen, W. L.; Maxwell, D. S.; Tirado-Rives, J. *J. Am. Chem. Soc.* **1996**, *118*, 11225–11236.
- (45) Canongia Lopes, J. N.; Pádua, A. A. H. *J. Phys. Chem. B* **2004**, *108*, 16893–16898.
- (46) Shimizu, K.; Almantariotis, D.; Costa Gomes, M. F.; Pádua, A. A. H.; Canongia Lopes, J. N. *J. Phys. Chem. B* **2010**, *114*, 3592–3600.
- (47) Bhargava, B. L.; Yasaka, Y.; Klein, M. L. *Chem. Commun.* **2011**, *47*, 6228–6241.